DNA double-strand breaks in heterochromatin elicit fast repair protein recruitment, histone H2AX phosphorylation and relocation to euchromatin

Burkhard Jakob[1], Jörn Splinter[1], Sandro Conrad[2], Kay-Obbe Voss[3], Daniele Zink[4], Marco Durante[1,5], Markus Löbrich[2,*] and Gisela Taucher-Scholz[1,*]

[1]Department of Biophysics, GSI Helmholtz Center for Heavy Ion Research, Planckstrasse 1, 64291 Darmstadt, [2]Radiation Biology and DNA Repair, Darmstadt University of Technology, Schnittspahnstrasse 13, 64287 Darmstadt, [3]Department of Materials Research, GSI Helmholtz Center for Heavy Ion Research, Planckstrasse 1, 64291 Darmstadt, Germany, [4]Institute of Bioengineering and Nanotechnology, 31 Biopolis Way, The Nanos 04-01, Singapore 138669 and [5]Institute for Condensed Matter Physics, Darmstadt University of Technology, 64289 Darmstadt, Germany

ABSTRACT

DNA double-strand breaks (DSBs) can induce chromosomal aberrations and carcinogenesis and their correct repair is crucial for genetic stability. The cellular response to DSBs depends on damage signaling including the phosphorylation of the histone H2AX (γH2AX). However, a lack of γH2AX formation in heterochromatin (HC) is generally observed after DNA damage induction. Here, we examine γH2AX and repair protein foci along linear ion tracks traversing heterochromatic regions in human or murine cells and find the DSBs and damage signal streaks bending around highly compacted DNA. Given the linear particle path, such bending indicates a relocation of damage from the initial induction site to the periphery of HC. Real-time imaging of the repair protein GFP-XRCC1 confirms fast recruitment to heterochromatic lesions inside murine chromocenters. Using single-ion microirradiation to induce localized DSBs directly within chromocenters, we demonstrate that H2AX is early phosphorylated within HC, but the damage site is subsequently expelled from the center to the periphery of chromocenters within ~20 min. While this process can occur in the absence of ATM kinase, the repair of DSBs bordering HC requires the protein. Finally, we describe a local decondensation of HC at the sites of ion hits, potentially allowing for DSB movement via physical forces.

INTRODUCTION

DNA double-strand breaks (DSBs) represent one of the most serious forms of DNA damage that can occur in the genome and their correct repair is critical for the avoidance of chromosomal translocations and cancer. DSBs can be induced either endogenously or by exogenous agents, e.g. ionizing radiation. In mammalian cells they evoke a coordinated multi-step response including damage recognition, signal transduction and repair. A central aspect of this response, important for genetic stability, is the phosphorylation of the histone variant H2AX (1,2), generating γH2AX, by the kinases ataxia telangiectasia mutated (ATM) (3) and DNA-PKcs (DNA-dependent protein kinase catalytic subunit) (4). Using immunofluorescent staining and microscopy, γH2AX appears as distinct ionizing radiation-induced foci (IRIF) around the DSB (5). Notwithstanding the expected homogeneous damage induction, various studies have indicated densely compacted heterochromatin (HC) to be refractory to H2AX phosphorylation, as no γH2AX IRIF could be detected in the center of heterochromatic regions in human cell lines between 15 min and 2 h following irradiation (6–9). Similar findings were reported for mouse embryonic fibroblast (MEF) cells, in which pericentromeric major satellite repeats are organized into readily visualized heterochromatic chromocenters showing dense DNA staining (10). Following DSB induction, γH2AX signals were absent from chromocenters 30 min after γ-irradiation (8,11) or neocarcinostatin treatment (12). In addition, in normal human fibroblasts and MEFs the radiation-induced DSBs associated with heterochromatic (11) or gene-poor pericentromeric regions (9) and chromocenters (8) have

---

been shown to be repaired with slower kinetics than DSBs in euchromatic DNA (13). Moreover, the repair of these breaks requires the concerted action of ATM and the mediator proteins, 53BP1, MDC1 and RNF8/168, to phosphorylate and inactivate the Krüppel-associated box (KRAB)-associated protein-1 (KAP-1), a HC building protein (8,11). An additional function of ATM is related to lesion complexity, which besides chromatin complexity can influence the speed of DSB repair (13, 14). This is especially relevant for ion-induced damage, since the densely ionizing charged particles are known to produce DSBs in close proximity leading to impaired repair and an increase in residual damage (15, 16).

To explain the notion of HC being a barrier to DSB repair, it has been postulated that the access of kinases to these highly compacted chromatin regions might be hindered (7,17). However, dextrans, whose size is comparable to DNA-PKcs and ATM, can access chromocenters directly without the need of damage signaling (18). Thus, the mechanism underlying the lack of γH2AX signal in heterochromatic regions is currently unclear. Here, we investigate the cellular response to DSBs in HC using heavy ion irradiation as a tool to deliver spatially localized DSBs (19). In MEF cells, we demonstrate that highly condensed chromocenters are directly accessible to efficient repair protein recruitment and H2AX phosphorylation at the DSBs, but the damage sites are subsequently relocated from the interior of HC to regions of lower chromatin density.

MATERIALS AND METHODS

Cell culture and transfection

Wild-type and ATM-deficient MEFs (MEFs and ATM$^{-/-}$-MEFs, respectively) were cultured in DMEM medium. HeLa cells stably expressing GFP-tagged histone H2B were grown in RP medium. All media (Biochrome) contained 10% FCS. For low angle ion irradiation cells were grown on coverslips or chambered cover glass (live cell microscopy). For single-ion irradiation cells were seeded on polypropylene foils as described (20). Double transfection of MEF cells with HP1α-Cherry and GFP-XRCC1 (kindly provided by Dr I. Müller, GSI, and Dr M. Lavin, Queensland Institute of Medical Research, respectively) was done by nucleofection using AMAXA (Lonza, Cologne) according to manufacturer's protocols.

Irradiation

Ion irradiation was done at the UNILAC or SIS accelerators at GSI as described (19). Ions (low energy <10 MeV/n unless stated otherwise) and their linear energy transfers (LETs): ^{12}C (200 keV/μm), ^{124}Xe (1 GeV/n high energy, 1350 keV/μm), ^{238}U (1 GeV/n high energy, 2000 keV/μm), ^{64}Ni (3430 keV/μm), ^{96}Ru (7060 keV/μm), ^{124}Xe (8680 keV/μm) and ^{238}U (14300 keV/μm). Note that the analysis of bending patterns is not affected by varying the ion species, since the patterns of the ion-induced γH2AX streaks are strikingly similar (21). For single-ion exposure, cells were pre-incubated (1 h) in medium with 0.1 μM Hoechst 33342 and irradiated in medium without phenol red including 1 mM HEPES as described (20). Cells were kept in the chamber for 30 min at the most. Ions (low energy $\sim$4.5 MeV/n) and their LETs: ^{12}C (290 keV/μm), ^{32}S (1560 keV/μm), 152Sm (9900 keV/μm) and ^{197}Au (12260 keV/μm). For details see Supplementary Figure S3.

Immunofluorescence staining

Cells were fixed in 2% formaldehyde and permeabilized as described (21). For end labeling of DSBs, after fixation and 10 min permeabilization the terminal deoxynucleotidyl transferase dUTP nick end labeling (TUNEL) assay was successively applied twice according to manufacturer's instructions (Roche). After blocking with 0.4% BSA in PBS, immunostaining was done as described above. It should be noted that 'dirty' ends are induced after ionizing radiation and thus not all DSBs induced are expected to be labeled. For repair kinetics in MEFs, cells were fixed 1 h in ice cold methanol and permeabilized 1 min in acetone before blocking and immunostaining. Mouse monoclonal antibodies anti-phospho-(Ser139)-H2AX (1:500, Upstate), anti-RPA (p34) (Lab Vision) and anti-ATM pS1981 (Rockland) at 1:200 and the rabbit polyclonal antibodies anti-XRCC1 (AHP 832; AbD Serotec) and anti-H3 trimethyl Lys9 (Upstate), both 1:500, were used in 0.4% BSA in PBS. Secondary antibodies were Alexa goat 488 and 568 anti-mouse F(ab)2 and anti-rabbit IgG conjugates (all Invitrogen). For DNA counterstaining either 1 μM ToPro3 or 3 μM DAPI was used.

Microscopy and image analysis

Image stacks were acquired using confocal microscopy (Leica TCS or Nikon spinning disk) using high NA oil immersion lenses. Image stacks were manually analyzed in 3D to define ion-hit chromocenters. For each time point 85–100 ion-hit chromocenters were analyzed. Image acquisition for γH2AX repair after carbon ion irradiation was performed using a Zeiss epifluorescence microscope. Acquired z-stacks were deconvolved using the Huygens essential software (SVI, Netherlands). Chromocenter- and euchromatin-associated γH2AX IRIF were enumerated in approximately 30 nuclei for each repair time point. All stack images consist of >20 slices with an increment of 0.2–0.28 μm. Live cell imaging after low angle exposure at the high energy SIS beamline was done essentially as described (22) but using an upgraded microscope (Olympus IX71 UPlanFL100x/1.3 1.6x Optovar) and EMCCD camera (Andor DU iXON+ 888). Image stacks, each consisting of two channels and 15 planes spaced by 400 nm, were recorded every 6.7 s.

RESULTS

Bending of linear ion-induced γH2AX tracks around heterochromatic regions

We first applied ion irradiation at low angle (19) to produce streak-shaped DNA-damage patterns

corresponding to the linear tracks of heavy ions across cell nuclei. These damage streaks allowed the reconstruction of the initial linear particle trajectories representing the primary sites of damage induction. We used human HeLa tumor cells stably expressing a GFP-tagged histone H2B to directly visualize chromatin density and immunostained for γH2AX 15 min after ion exposure. We reproducibly found γH2AX streaks bending at regions of high chromatin density as shown for perinucleolar HC (Figure 1a). Considering the linearity of the charged particle path within the cell, this bending suggested a displacement of the phosphorylated damage site relative to the initially induced DSB location. To confirm this observation in cell nuclei with larger heterochromatic compartments, we next exposed MEFs to low-angle ion irradiation allowing to discriminate hit and non-hit chromocenters. The ion-hit chromocenters frequently showed γH2AX signals bent around their borders (Figure 1b and c). Such bending patterns were also observed for the damage response protein XRCC1 and the ssDNA marker Replication Protein A (RPA) (Supplementary Figure S1). The deviations from linearity detected along ion-induced streaks of RPA or γH2AX foci could be allocated to H3K9me3-stained heterochromatic compartments (Supplementary Figure S1C and D). Major structural changes of these compartments upon ion irradiation were not apparent.

The detected bending patterns are in line with the previously observed exclusion of γH2AX from HC, but given the linearity of the charged particle path in matter they also indicate a relocation of the damage from the initial induction site in the interior of the HC compartment to its periphery. The direction of this relocation can vary from either perpendicular to the ion traversal (Figure 1d), resulting in a bent pattern, or along the ion trajectory, forming an interrupted streak (Figure 1e). Also weak γH2AX signals within chromocenters were sometimes found (Figure 1f). The relative frequencies of external and internal signals were analyzed for different time points post-irradiation. At the earliest observation time of 15 min, already 71 ± 7% of the ion-hit chromocenters showed external signals. Accordingly, only 29 ± 5% exhibited internal signals (Figure 1g). The relocation process appeared to be almost complete 1 h after damage induction, because there was no significant difference in the frequency of internal γH2AX signals between 1 h (16%) and 4 h (12%) post-irradiation (Figure 1g).

Damage response proteins and γH2AX remain co-localized with the DNA break sites

In order to exclude that γH2AX and/or the repair proteins analyzed could be drifted independently of the DNA damage, we checked the co-localization of protein foci with the induced DSBs at 5 and 30 min post-irradiation of MEF cells. Taking advantage of the production of multiple DSBs in close proximity by heavy ions, we used a modified TUNEL assay to end-label the free DNA ends and directly visualize the induced DSBs co-stained with damage markers. DSBs were found co-localizing with γH2AX and the repair factors XRCC1 or RPA at all
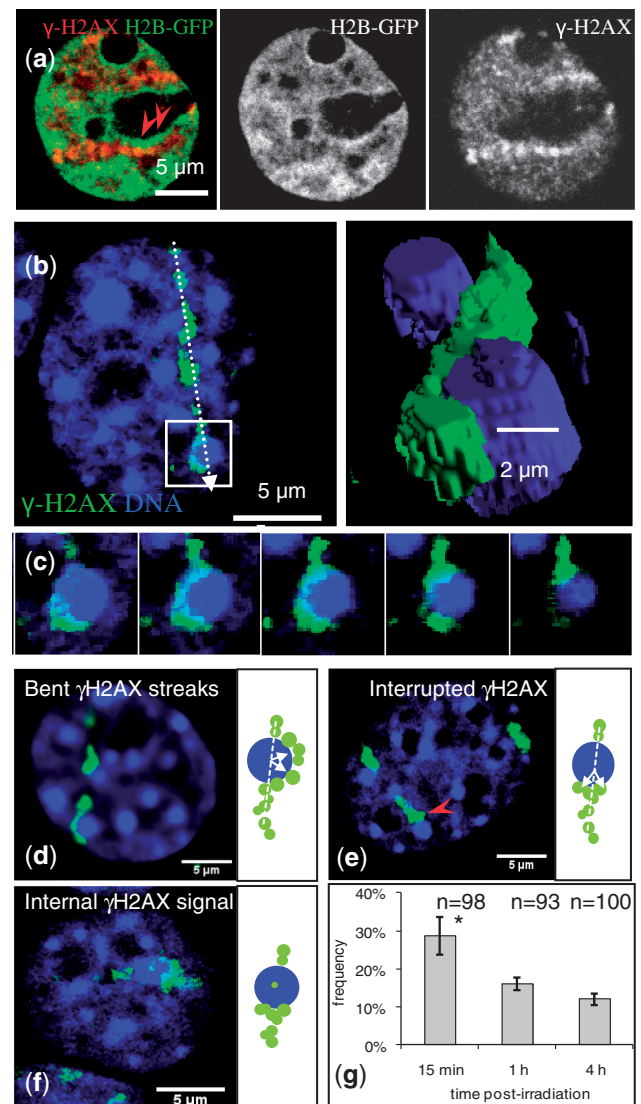

Figure 1. Bending of linear ion-induced γH2AX streaks indicates chromatin density-dependent damage relocation. (**a**) HeLa cells expressing GFP-tagged histone H2B were nickel ion-irradiated at low angle and immunostained for γH2AX after 15 min. Left image (merged): Chromatin is visualized by H2B-GFP (green), brighter staining indicating higher density as observed around nucleoli (red arrowheads). The depicted linear γH2AX streaks (red) show a slight but consistent bending following the course of bright perinucleolar chromatin staining. Separate channels are shown on the right. (**b**) Single slice image of a MEF nucleus irradiated with xenon ions to induce linear damage streaks visualized by γH2AX (green) 1 h post-irradiation. Intense DNA-stained regions (DAPI; blue) represent heterochromatic compartments (chromocenters), as confirmed by histone H3-K9me3 staining (Supplementary Figure S1A). The original ion track (arrow) was derived from 3D analysis of the confocal image stack allowing interpolation of the γH2AX streak. Chromocenters traversed by the interpolated trajectory were defined as ion-hit. 3D analysis is exemplarily shown for an ion-hit chromocenter as a rendered 3D-image (right panel) and (**c**) as a montage of different z-planes (Δ = 0.2 μm). Three types of γH2AX patterns, each shown in a MEF nucleus and as a schematic drawing, were observed at ion-hit chromocenters: bent streaks (**d**), interrupted streaks (**e**) and internal signals (**f**). Bent and interrupted streaks represent external signals, only distinguished by the direction of damage translocation indicated by arrows in the schemes (d and e). (**g**) Distribution of internal signals over time post-irradiation. Internal γH2AX signals within ion-hit chromocenters were significantly reduced from 15 min to 1 h post-irradiation ($P < 0.05$ using *t*-test; asterisk). Error bars represent the SEM of four independent experiments, *n* is the number of analyzed ion-hit chromocenters.

time points analyzed, independent of the location of the damage response foci (Figure 2). This demonstrates that the damage markers remain stably located on the chromosome relative to the break site. In support of a relocation of DNA lesions with time, internal free DNA ends were clearly detected within some of the ion-hit chromocenters 5 min after irradiation (Figure 2a and b; Supplementary Figure S2), whereas at 30 min both the *in situ* labeled DSBs and the co-stained damage response proteins always appeared external, often bending around the heterochromatic compartments (Figure 2c and d). We did not observe H2AX phosphorylation within chromocenters in response to nearby passing DSB tracks (Figure 2e), indicating a lack of γH2AX spreading towards neighboring condensed chromatin regions, in agreement with findings described for endonuclease-mediated DSBs in yeast (12).

Fast recruitment of damage response proteins within HC

To confirm the accessibility of HC to DNA repair factors, we measured the recruitment of GFP-tagged XRCC1 to ion-induced lesions directly during irradiation of MEFs using live cell microscopy (23,24). Time-lapse images of hit chromocenters containing the Cherry-tagged HC protein HP1α for visualization show the fast accumulation of GFP-XRCC1 to IRIF along the straight ion track both within and outside the HC compartment (Figure 3a and Supplementary Movies S1–S3). Remarkably, the recruitment kinetics was very fast independent of chromatin density, but the release of the protein was significantly delayed within HC compared to euchromatic regions (Figure 3a and b). This could be related to impaired processing of heterochromatic lesions, as reported for HC DSB repair (8). As shown in the movies, we also observed a non-directional, billowing motion of the damage tracks suggesting their drift to the periphery. In this linear track irradiation set-up, the low random hitting frequency of chromocenters and the limited time span for live cell imaging of XRCC1 foci preclude a direct visualization of the relocation process. In addition, while moving within HC a bending of damage streaks was not observed, suggesting that it is induced at a later time in consequence of the emergence of damaged chromatin to the HC boundary surface.

Damage response and rapid relocation of DSBs induced centrally within heterochromatic compartments

To improve chromocenter hitting and to allow for statistical analysis, we next analyzed the early DSB dynamics utilizing the heavy ion microprobe. The unique submicrometer resolution of the GSI microbeam (20) enabled the aimed irradiation of subnuclear compartments like chromocenters (typically ~1–2 μm in diameter) with single ions as specified in Supplementary Figure S3. MEF nuclei were stained with the vital dye Hoechst 33342 and chromocenters were manually targeted (red crosses in Figure 4a) using a microscope. Multiple fields of view containing up to 100 cells each were selected for ion exposure. The irradiation of one field took 3 s at most and several fields per sample were
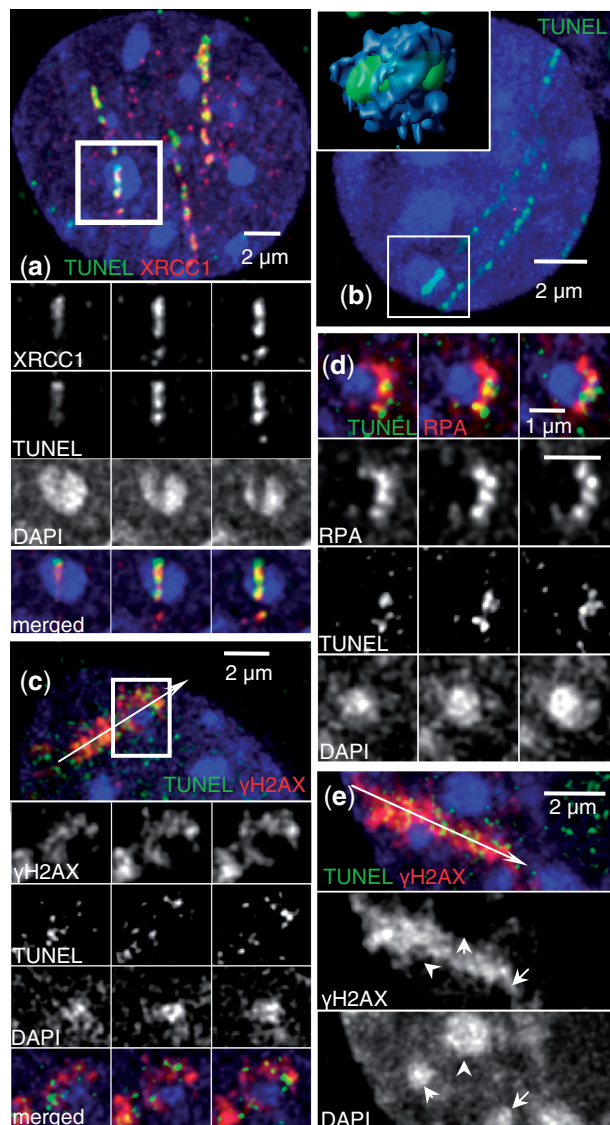

Figure 2. Damage markers remain co-localized with break sites bending around HC. Shown are streaks of directly visualized DSBs (green, labeled by TUNEL) along uranium ion tracks in MEF nuclei. Chromocenters are indicated by intense DAPI staining (blue) (**a**) Merged projection image (top) showing DSBs (green) co-localizing with the damage marker XRCC1 (red) 5 min post-irradiation. Bottom: selected confocal slices indicating the internal location of DSBs within the traversed chromocenter (box). Shown are the separate color channels and the merged image. (**b**) DSBs (green) located within HC 5 min post-irradiation (box). The insert shows the corresponding 3D surface image. (**c**) DSBs co-stained with γH2AX (red) are depicted in the merged projection image (top) and selected confocal slices (bottom, separate channels and merged) demonstrating the bending of the DSB streak around heterochromatic regions and the co-localization with γH2AX at 30 min post-irradiation. The arrow in the upper image indicates the reconstructed original ion track crossing the chromocenter. (**d**) DSBs co-localizing with RPA (red) at the periphery of a chromocenter are depicted in single confocal slices 30 min after ion exposure as merged image (top) or separate channels below. (**e**) Ion track passing nearby chromocenters (arrow) with γH2AX staining (red) 30 min post-irradiation showing that chromocenters are precluded from γH2AX spreading. Separate channels of γH2AX and DAPI are depicted below. White arrowheads indicate the border of three bypassed chromocenters that form a barrier for the propagation of the γH2AX signal.
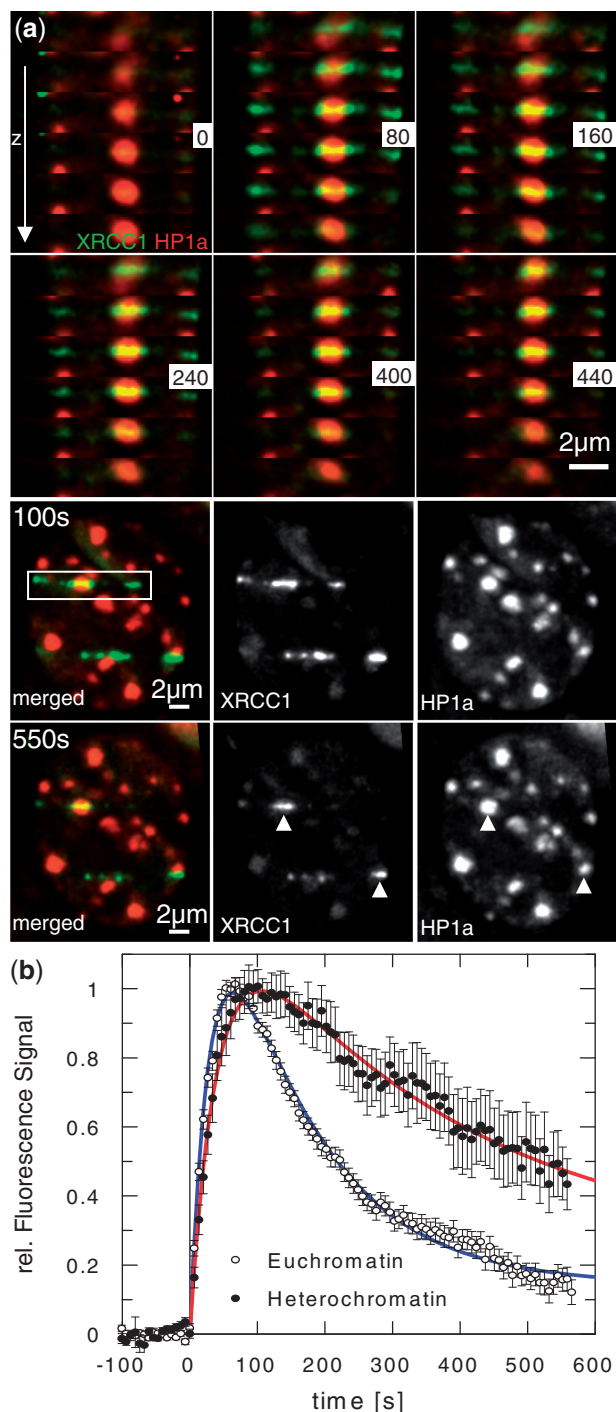
Figure 3. Fast recruitment of the repair protein XRCC1 to heterochromatic DNA damage. (**a**) Live cell imaging at the high energy beamline showing the recruitment of GFP-XRCC1 (green) to linear 1 GeV/u uranium ion-induced tracks traversing hetero (HC)- and euchromatic (EC) regions in MEF nuclei. Chromocenters are marked by co-expression of HC-associated Cherry-tagged HP1α (red). Top: depicted are selected image stacks (times in seconds as indicated in the inset) of one centrally hit chromocenter and three EC-foci along the ion track. Each time frame is displayed as six central consecutive z-slices of the image stacks acquired. The shift of the brightest HC-associated XRCC1 signals at 160 s to upper z-slices at 440 s indicates movement to the chromocenter top. Bottom: projection image of the whole nucleus 100 s (upper row) and 550 s after irradiation showing the preferential loss of the euchromatic XRCC1 signal. The box indicates the area from which the z-slices are taken. On the right, the

successively irradiated with time lags of 1–3 min. Since all cells within a sample were then fixed at once, each field represents a different post-irradiation time point.

Ion-induced DNA damage was visualized by immunostaining against γH2AX and XRCC1. Representative light-optical sections of ion-induced γH2AX and XRCC1 foci are shown for samples at 5 and 7 min after irradiation of chromocenters with 4.5 MeV/u sulfur or gold ions, respectively (Figure 4 and Supplementary Figure S3). At these early time points, we observed internal XRCC1 foci in 2/3 of the ion-hit chromocenters. The XRCC1 signals co-localized with γH2AX (Figure 4a) and ATMpS1981 (Supplementary Figure S3), the activated ATM protein (25). The results demonstrate that, in contrast to previous assumptions (7, 17), H2AX is phosphorylated within HC at early times post-irradiation. This response was obtained in plateau phase cells and is thus not restricted to late S-phase, as previously reported for MCF7 cells (7).

XRCC1 co-localizes with γH2AX at the induced DSBs but forms comparatively smaller IRIF (24,26) and is thus useful for monitoring the short-range damage relocation at early times. Three different types of XRCC1 focus positions were defined relative to the targeted chromocenter considering the intensity profile of the surrounding DNA signal: centrally, intermediately and peripherally located IRIF (Figure 4b). For centrally located foci, the XRCC1 signal peak was totally enclosed by a bright DNA staining independent of the direction of the profile (Figure 4b; top panel). Intermediately located foci always exhibited direction-dependent intensity profiles either enclosing or flanking the signal. (Figure 4b, mid panel). Expelled foci were generally flanking bright chromocenter DNA staining and additionally revealed bent signals in the 3D analysis (Figure 4b, bottom panel). Bending of signal patterns was the recognition feature for initially central ion hits and only these were defined as 'completely expelled'. Foci adjacent to chromocenters that did not show any bending were considered to be off-target and were not included in the analysis. The relative frequency of each position was calculated for the first 20 min following single-ion irradiation and the data were pooled in three time intervals. The fraction of ion-hit chromocenters with centrally located XRCC1 signals decreased from $28 \pm 8\%$ at 3–8 min post-irradiation to $8 \pm 5\%$ for the time period of 9–13 min and to ~2% for the latest time interval from 14 to 20 min (Figure 4c). This significant time-dependent reduction of centrally located foci clearly demonstrates the dynamic relocation process. Within the same time period, the relative frequency of peripheral IRIF increased from $34 \pm 3\%$ to $70 \pm 4\%$ (Figure 4c), proving that XRCC1

Figure 3. Continued

separate channels (XRCC1 and HP1α) are shown. The total observation time of ~10 min is shown in the Supplementary Movies for this (Movie S1, nucleus turned by 90°) and another nucleus with a hit chromocenter (Supplementary Movies S2 and S3). (**b**) Kinetics of GFP-XRCC1 recruitment in HC (18 foci) and EC (78 foci) measured as described in (a) and fitted by exponential functions. Error bars indicate SEM.
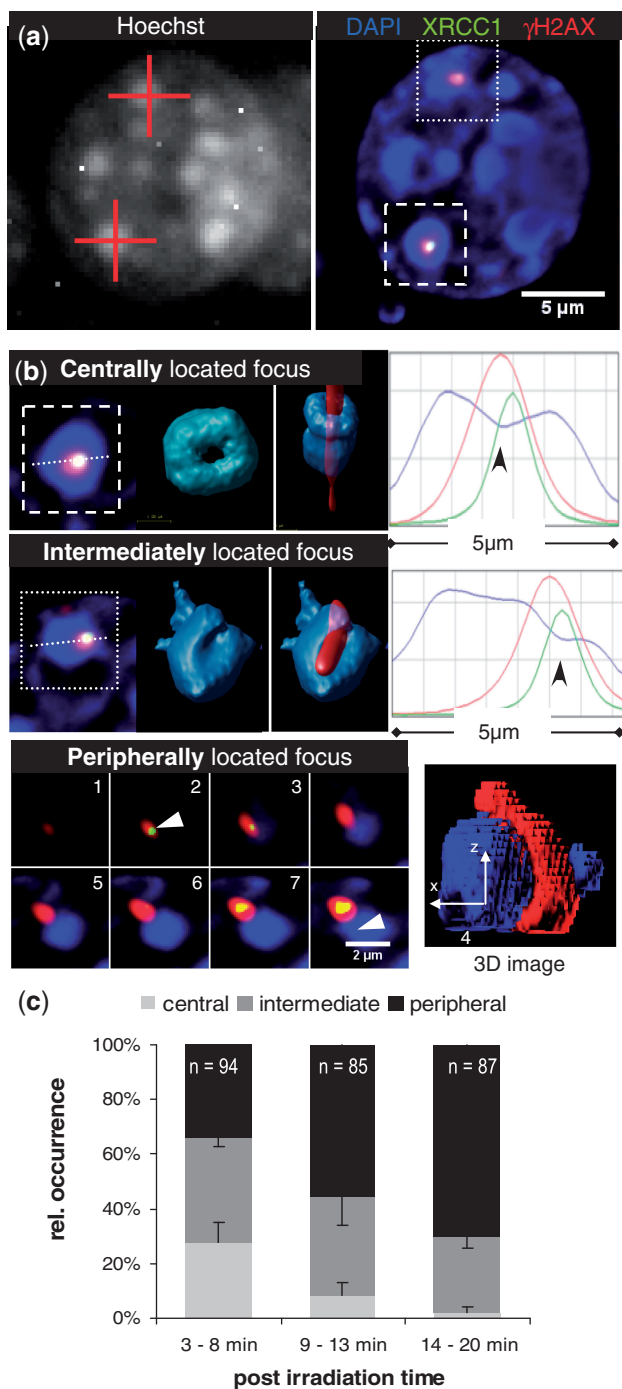
signals initially located in the center move to the chromocenters' border within the first 20 min following irradiation.

Even in the earliest period (3–8 min), centrally and intermediately located XRCC1 signals represented only 66% of the ion-hit chromocenters (Figure 4c) indicating that the damage relocation had already affected the position of the damage site at these early time points. This notion is further supported by the occasional bending of *in situ* labeled DSBs observed 5 min after low angle ion irradiation (Supplementary Figure S2). At later times (14–20 min) central and intermediate signals were less frequently observed (~30%) consistent with the frequency of internal signals found 15 min after low angle ion irradiation (Figure 1g).

Remarkably, despite the fact that ion irradiation induces several DSBs within a single chromocenter (e.g. ~20 DSBs by one sulfur ion; calculated as described in 19), damage patterns representing differential movement of the individual breaks to the periphery, such as halo signals completely surrounding the ion-hit compartments, were extremely rare (one out of 266 analyzed chromocenters).

Repair of complex DSBs adjoining HC is delayed and ATM dependent

Emerging evidence suggests that DSBs repaired with slow kinetics and requiring ATM are predominantly localized at the edge of HC (8,13). In light of our finding that DSBs on the periphery of HC at later times (>15 min) post-irradiation represent breaks which were mainly induced inside HC and subsequently expelled, we tested whether these breaks are also repaired in an ATM-dependent manner and with slower kinetics. For this, we used the low-angle irradiation set-up allowing the visualization

Figure 4. Relocation dynamics of damage sites centrally induced within chromocenters. The MEF nucleus was irradiated with single sulfur ions and immunostained 5 min post-irradiation. For details of microbeam targeting see Figure S3 (**a**) H2AX is phosphorylated and XRCC1 accumulates at heterochromatic DSBs directly after single-ion irradiation. The left-hand image shows the aimed targeting of chromocenters (red crosses) for single-ion irradiation using Hoechst 33342 (grey scale) as a marker in nuclei of living MEF cells. The right-hand image shows the same nucleus after fixation at 5 min post-irradiation. DNA damage-induced foci of the repair factor XRCC1 (green) and γH2AX (red) are clearly visualized at the sites of ion traversal. Both proteins co-localize within each of the targeted chromocenters (blue: DAPI DNA staining). (**b**) Definition of different radiation-induced foci positions relative to the ion-hit chromocenter. The depicted hit MEF chromocenters [marked boxes in (a), right panel] stained as detailed above upper panel: co-localizing XRCC1

Figure 4. Continued
and γH2AX IRIF are centrally located within a chromocenter as illustrated in the projection (left) and corresponding rendered surface images for γH2AX and DAPI (mid images). The intensity profile measured along the respective dotted line in the single slice image indicates that DNA staining (blue) is depleted (black arrows) at the damage site marked by XRCC1 (green) and γH2AX (red). The depleted DNA staining intensity co-localizes with the damage markers. Mid panel: co-localizing XRCC1 and γH2AX IRIF are located off-centered within the chromocenter (rendered surface images, mid images) defining the IRIF as intermediately located. The intensity profile measured as above shows the depleted DNA staining (blue) co-localizing with the damage markers (green and red) also at the intermediate position. Lower panels: gallery of consecutive light-optical sections (Δ = 0.2 μm) showing the xy position of the damage sites marked by XRCC1 and γH2AX foci. Arrowheads (Frames 2 and 8) mark the initial positions of the damage induced at the ion traversal. The displacement between the damage (foci) and its original induction site (arrowhead) shown in Frame 8 demonstrates the relocation of the damage from the center to the periphery of the chromocenter. The resulting bending of the γH2AX signal surrounding the chromocenter is additionally shown in a rendered 3D image. (**c**) Analysis of the time-dependent localization of XRCC1 and γH2AX IRIF (positions defined in b). Relative frequencies of each position are given for the indicated post-irradiation intervals and (*n*), the total number of ion-hit chromocenters from three independent experiments, is indicated. Error bars represent the SEM.
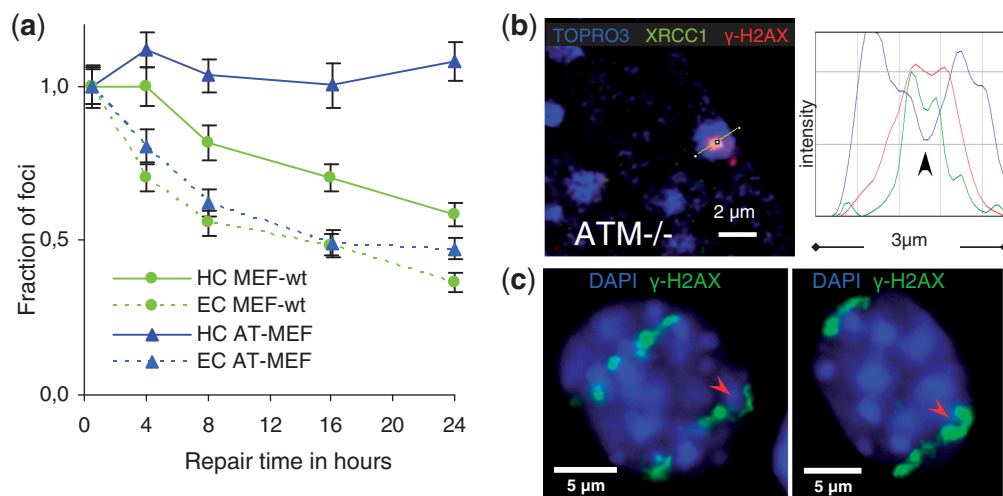
Figure 5. Chromatin-density and absence of ATM influence the repair kinetics of carbon ion-induced DSBs. (**a**) Normalized repair kinetics for γH2AX foci following low angle carbon ion irradiation. The number of γH2AX foci was enumerated in G1 phase wild-type (green) and ATM$^{-/-}$ MEF cells (blue) at the indicated time points after ion exposure. γH2AX signals exhibiting distinct maxima were counted as individual foci. Foci were discriminated to be either associated with the intensively DAPI stained heterochromatic chromocenters (HC) or with euchromatic regions (EC) using software-aided visual inspection. Only foci directly adjacent to HC are classified as being HC-associated, and signals spatially separated are classified EC-associated. At 30 min post-irradiation about 1/3 of the foci were found associated with HC. Repair of HC-associated damages in wt-MEFs (solid green line) is delayed compared to EC-associated DSBs in either wt MEFs (dashed green line) or ATM$^{-/-}$ MEFs (dashed blue line), whereas in ATM$^{-/-}$ MEFs the repair of HC-associated DSBs is abolished (solid blue line). For each time point ~30 nuclei were analyzed. Error bars represent the SEM. (**b**) ATM is not required for the damage response within HC. ATM$^{-/-}$ MEF nucleus (left) targeted with a single samarium ion at the microprobe. The hit chromocenter shows XRCC1 (green) recruitment and γH2AX (red) formation within highly compacted DNA (blue: ToPro3). The intensity profile (right panel) measured along the dotted line in the single slice image of the chromocenter shows depleted DNA staining at the damage site (black arrows). (**c**) Depicted ATM$^{-/-}$ MEF nuclei were carbon ion irradiated at low angle. Staining for γH2AX (green) shows bending patterns around ion-hit chromocenters 30 min post-irradiation. DNA was stained using DAPI (blue).

and counting of individual γH2AX foci along the damage streaks.

We subdivided carbon ion-induced IRIF into chromocenter- and euchromatin (EC)-associated foci in MEFs and assessed DSB repair kinetics in these distinct chromatin compartments (Figure 5a). Consistent with an influence of damage complexity on DSB repair, EC-associated γH2AX foci were repaired with slow kinetics, similar to the repair of DSBs in normal human fibroblasts following heavy ion irradiation with the same or comparable lesion density (16,27). However, the repair of chromocenter-associated DSBs was significantly slower during the first 4 h post-irradiation. Similar results were obtained by measuring the length of the streak-shaped γH2AX signals associated with chromocenters instead of counting IRIF (Supplementary Figure S4). At later time points, no significant difference in the repair kinetics of EC- and chromocenter-associated DSBs was observed. We also analyzed ATM$^{-/-}$ MEFs and obtained repair kinetics for euchromatic DSBs similar to those of wt-MEFs (Figure 5a). However, ATM$^{-/-}$ MEFs showed a complete lack of repair for chromocenter-associated foci indicating that ATM is required for the repair of those DSBs that were induced by carbon ions inside HC and subsequently expelled to the periphery. In line with this hypothesis, phosphorylated H2AX was clearly evident in ATM$^{-/-}$-MEF cells 3 min after centrally hitting the chromocenters using targeted single-ion irradiation (Figure 5b). Furthermore, since ATM's function during heterochromatic DSB repair involves HC relaxation

(8,28), we tested for signs of damage relocation in ATM knockout cells after low-angle carbon irradiation. Bent signal patterns similar to those of wt-MEFs were clearly observed 30 min after damage induction in ATM$^{-/-}$ MEFs (Figure 5c), suggesting that the relocation of HC-associated DSBs is largely independent of the kinase.

Local decondensation of HC at sites of DNA damage

Aimed at gaining insight into the mechanism underlying heterochromatic damage movement we speculated that a damage-induced local chromatin decondensation, as recently reported after ultraviolet A (UVA) laser micro-irradiation (29), could create alterations in the balance of physical forces inside a confined heterochromatic compartment resulting in a driving force for motion. Here, we analyzed the DNA staining patterns after single-ion irradiation and observed significantly depleted ToPro3 or DAPI signals at the sites of ion hits (Figures 4b, 6a and b), suggesting a local decondensation of chromatin. To exclude the possibility that the decreased staining was somehow related to DNA disruption, we irradiated MEF cells with low energy ions and measured Hoechst 33342 staining in hit chromocenters in real time at the beamline microscope. The continuous but not instantaneous decrease of DNA staining intensity observed in ion-hit but not in unirradiated chromocenters during live cell imaging over ~3 min (Figure 6c–e) supports a physiological decondensation process. In addition, the signal
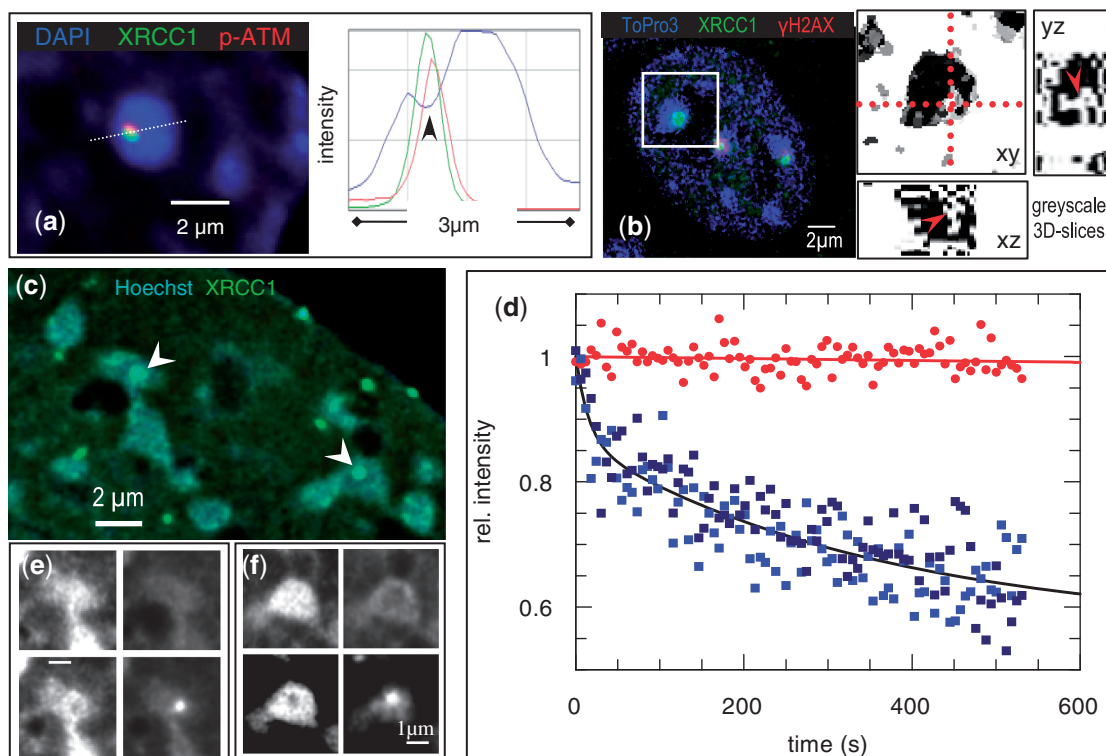
Figure 6. Decondensation of heterochromatic DNA in MEF chromocenters traversed by low energy ions. (**a**) Chromocenter of a MEF nucleus immunostained 7 min after targeted irradiation with single sulfur ions. Image of the ion-hit chromocenter (left) and intensity profile (right) along the dotted line showing depleted DNA (DAPI) staining (blue) at the damage site marked by XRCC1 (green) and p-ATM (red) marked by black arrow. (**b**) 3D analysis of a gold ion-hit chromocenter (box) showing depleted DNA staining along the whole ion traversal (red arrows within the binary threshold 3D-slice images; red dotted lines indicate the positions of the depicted xz- and yz-plane). Note that in (a) and (b), independent of the DNA stain and the ion species, the depleted DNA staining intensity clearly co-localizes with the damage markers. (**c**) Real-time decondensation of uranium-hit chromocenters was measured in a living MEF by local depletion of DNA-bound Hoechst 33342 fluorescence. Sites of ion traversal are indicated by GFP-XRCC1 accumulation (green). (**d**) Two centrally hit chromocenters (white arrows in c) were individually analyzed (blue symbols and line) in a central projection of a 3D-data set. For comparison, the mean values for three non-hit chromocenter are shown (red symbols; red line). Fluorescence intensity was corrected for bleaching and normalized to the initial intensity. The continuous fluorescence decline at the hit HC site indicates a biological decondensation process, ruling out an instantaneous DNA staining depletion related to disruption of the DNA or Hoechst dye due to particle traversal. (**e** and **f**) Images of the two chromocenters analyzed in (d) before (upper panels) and 4 min after ion traversal (bottom panels). Depicted are the Hoechst 33342 stained DNA (left panels) and the XRCC1 fluorescence (right panels) for each chromocenter in (e) and (f), respectively. Besides depletion of the DNA staining, major structural alterations of the chromocenters are not apparent.

depletion observed after targeted chromocenter irradiation both at centrally and intermediately located IRIF (Figure 4b) suggests that the decondensed chromatin regions were also relocated from the interior to the periphery of ion-hit chromocenters.

DISCUSSION

Recently a number of studies have suggested that HC may be a barrier to IRIF formation, although DSBs are homogenously induced also in highly compacted DNA (13). The preferential localization of γH2AX signals at euchromatic regions observed in our study at 15 min and later after ion-induced DNA damage agrees with these previous measurements using sparsely ionizing radiation [15 min (9), 30 min (7,8,11) or 1 h (6,11) post-irradiation] or neocarcinostatin [after 1 h treatment; (12)]. A recent report following irradiation with 1 GeV/n iron ions describes a significantly preferred localization of IRIF at the border of intensively stained DNA regions that was

suggestive of a small range translocation of the damage sites (30). In the present study, we provide direct experimental evidence for a chromatin density-dependent relocation process that explains these previous findings.

The most striking observation arising from our analysis of ion-induced damage tracks is that γH2AX foci streaks bordering HC regions were bent. Given the linearity of the physical particle path, we attribute the curvature to the movement of foci to the HC borders outside the initial ion path. By detecting DSBs directly and showing their strict co-localization with damage markers including γH2AX, we demonstrate that the foci formed on damaged chromatin are not independently rearranged. Furthermore, as DSBs were found inside HC at early (5 min) but not at later times (>30 min) after low angle irradiation, when bending was observed, we provide evidence for a time-dependent relocation of the breaks to the periphery. At the same time, γH2AX spreading over time does not occur toward the interior of HC, as linear damage streaks randomly induced nearby

chromocenters remain outside, in agreement with the studies cited above (13). The partially internal γH2AX signals we observed even hours after irradiation might correspond to parts of the γH2AX stained domain flanking the actual break sites about one Mbp up- and down-stream (31,32). In line with this assumption, we frequently observed that, although the DSBs and the co-localizing XRCC1 or RPA signals were clearly expelled from the chromocenter, the γH2AX signal was broader and in part overlapping toward the interior (Figure 2c).

To elucidate the time course of damage site relocation, we used aimed single-ion irradiation. This allowed us to induce DSBs in the center of HC compartments with the same submicrometer targeting accuracy for all hit chromocenters (independent of the time of analysis). The reproducible increase of peripherically located (bent) tracks with time post-irradiation demonstrates that the damage sites initially induced within HC are expelled to lower chromatin density regions. Within the 20 min time period monitored relocation occurred in about 30% of the cells. However, already at the earliest interval (3–8 min) about one-third of the XRCC1 signals were external. The analysis of linear tracks further suggests that the relocation process goes on beyond 20 min. More detailed time course studies will reveal whether over time, as we presume, all HC-associated foci are moved outside.

Informatively, curved damage tracks were observed around the border of HC regions but never inside, suggesting a connection to the spherical shape of the chromocenter surface.

Recently, it has been proposed that both damage and chromatin complexity can influence the kinetics of DSB repair (13,27). Following γ-irradiation of normal human fibroblasts and MEFs the repair of HC-associated DSBs has been reported to be slower than that of euchromatic breaks and dependent on ATM (8,17). In addition, a regulatory role of ATM in DSB end resection has proposed to be relevant for the repair of complex DSBs in G2 phase (27). However, EC-associated DSBs after X-rays do not require ATM for their repair (8). Here, we show that the repair of complex euchromatic DSBs induced by carbon ions in G1 MEF cells is also independent of ATM (Figure 5). Nonetheless, the DSBs arising in EC-DNA after carbon ion irradiation are repaired with slow kinetics, similar to the one obtained previously following exposure of G1 human fibroblasts to the same densely ionizing radiation type (27). HC poses an additional barrier to DSB repair in this system, as delayed repair of HC-associated DSBs was measured after carbon ion irradiation in wt-MEFs. Remarkably, in ATM$^{-/-}$ MEFs the repair of chromocenter-associated foci was completely abolished. We note that ion-induced foci do not necessarily represent single DSBs due to lesion clustering (15,33). Therefore, foci loss kinetics may not represent the time course of the repair of individual DSBs. Notwithstanding this limitation, the pronounced difference in HC-foci loss between ATM$^{-/-}$ and wt cells is not explained by lesion clustering. Rather, the observed ATM-dependent repair of HC-DSBs is consistent with a role of ATM in chromatin relaxation via phosphorylation

of KAP1 (8,28). Furthermore, our results suggest that the DSBs localized on the periphery of HC, which are repaired in an ATM-dependent manner, are those expelled from the interior of heterochromatic regions. Thus, it is likely that DSBs induced by γ-irradiation which localize adjacent to heterochromatic regions and require ATM for repair (8) also represent breaks initially induced inside HC. The relocation process does not appear to require ATM, but in the absence of ATM these breaks remain unrepaired at the periphery of HC. Since cells deficient in 53BP1, MDC1 and RNF8/168 also exhibit unrepaired DSBs at the border of HC (11), it is likely that these mediators of the ATM signaling response are equally dispensable for the relocation process. Indeed, a genetic requirement for this process has yet not been determined (13). It seems possible that ATM and the signaling mediators are needed during the relocation process to maintain the fine structure of the chromatin surrounding DSBs, a function which might be necessary for the repair of these lesions. It is, however, unlikely that HC structure is significantly altered by the presence of ion-induced DSBs, as based on H3K9me3 immunostaining or real-time imaging major chromocenter rearrangements are not apparent (Figure 6 and Supplementary Figure S1). Consistent with this notion, ATM is still required for the repair of carbon ion-induced HC-DSBs, comparable to X-rays (8).

The mechanism of DSB movement is not yet clear, but in consideration of our results it is tempting to speculate that it is physically driven rather than enzyme mediated. A local relaxation of nucleosome compaction could be induced in the case of discrete ion irradiation, as supported by the DNA decondensation observed at sites of ion traversal in real-time imaging and in microirradiation experiments (Figures 6 and 4). This presumably creates significant alterations in the balance of physical forces inside a heterochromatic compartment. Also, following UVA laser microirradiation a damage induced, locally confined chromatin decondensation has been reported, which was independent of ATM and γH2AX (29). A local chromatin decondensation appearing as a protrusion of damage signals into lower density chromatin was as well-described after exposure of human cells to γ-rays, and the decreased chromatin staining intensities were related to changes in histone modifications (34).

A configuration of relaxed chromatin enclosed by highly compacted HC is energetically disadvantageous, and the resulting net forces could drive the relocation process. Such forces holding together the decondensed domains would also explain the observed concerted relocation of the multiple DSBs that are nearby produced by ion microirradiation. Further support for a physically driven relocation arises from a recent study indicating that entropic forces resulting from the self-governed biophysical process of macromolecular crowding can promote and stabilize self-organization of chromocenters at low cellular energy costs and without the need for discrete boundaries such as membranes (18).

We and others have established that damaged chromatin domains do not undergo large-scale movement in the nucleus, independent of the type of insult (23,35). The

small-scale DSB relocation shown here in HC is compatible with the prevailing concept of positional DSB stability. We suggest that the damaged domains defined by decreased compaction undergo a non-directional migration within condensed DNA (Movie S2). Considering the dimension of chromocenters, a 20 min period appears sufficient for random migration of the decondensed chromatin region to the HC border assuming normal (global) chromatin diffusion rates, while the opposite drift is hampered by the low diffusion coefficient of the heterochromatic compartment compared to euchromatin (18). Therefore, once at the periphery, damage foci could lead to the random accumulation of the lesions at the boundaries of HC. Direct support for the DSB movement is given by a very recent publication reporting the expansion and dynamic protrusion of heterochromatic repetitive DNA in *Drosophila* after ionizing radiation before undergoing homologous recombination repair (36). Considering the different organization of fruit fly chromatin and the differences in chromatin structure between murine and human cells the common observation of DSB movement to the periphery of heterochromatic compartments points to a general phenomenon in the repair of heterochromatic DNA lesions.

Taken together, we have demonstrated that HC DSBs in mammalian cells, in contrast to the common belief, induce phosphorylation of H2AX and fast recruitment of repair proteins. Lesions then move from the interior to the periphery of irradiated heterochromatic compartments within ~20 min post-irradiation. In addition, we show a local decondensation of HC at the sites of ion hits potentially promoting the movement of DSBs to the HC periphery where repair may proceed.

SUPPLEMENTARY DATA

Supplementary Data are available at NAR Online.

ACKNOWLEDGEMENTS

FUNDING

REFERENCES

1. Celeste,A., Petersen,S., Romanienko,P.J., Fernandez-Capetillo,O., Chen,H.T., Sedelnikova,O.A., Reina-San-Martin,B., Coppola,V., Meffre,E., Difilippantonio,M.J. *et al.* (2002) Genomic instability in mice lacking histone H2AX. *Science*, **296**, 922–927.
2. Bassing,C.H., Chua,K.F., Sekiguchi,J., Suh,H., Whitlow,S.R., Fleming,J.C., Monroe,B.C., Yan,C., Vlasakova,K. *et al.* (2002) Increased ionizing radiation sensitivity and genomic instability in the absence of histone H2AX. *Proc. Natl. Acad. Sci. USA*, **99**, 8173–8178.
3. Burma,S., Chen,B.P., Murphy,M., Kurimasa,A. and Chen,D.J. (2001) ATM phosphorylates histone H2AX in response to DNA double-strand breaks. *J. Biol. Chem.*, **276**, 42462–42467.
4. Stiff,T., O'Driscoll,M., Rief,N., Iwabuchi,K., Löbrich,M. and Jeggo,P.A. (2004) ATM and DNA-PK function redundantly to phosphorylate H2AX after exposure to ionizing radiation. *Cancer Res.*, **64**, 2390–2396.
5. Rogakou,E.P., Boon,C., Redon,C. and Bonner,W.M. (1999) Megabase chromatin domains involved in DNA double-strand breaks in vivo. *J. Cell Biol.*, **146**, 905–916.
6. Vasireddy,R.S., Karagiannis,T.C. and El-Osta,A. (2010) γ-radiation-induced γH2AX formation occurs preferentially in actively transcribed euchromatic loci. *Cell. Mol. Life Sci.*, **67**, 291–294.
7. Cowell,I.G., Sunter,N.J., Singh,P.B., Austin,C.A., Durkacz,B.W. and Tilby,M.J. (2007) γH2AX foci form preferentially in euchromatin after ionising-radiation. *PLoS One*, **2**, e1057.
8. Goodarzi,A.A., Noon,A.T., Deckbar,D., Ziv,Y., Shiloh,Y., Löbrich,M. and Jeggo,P.A. (2008) ATM signaling facilitates repair of DNA double-strand breaks associated with heterochromatin. *Mol. Cell*, **31**, 167–177.
9. Falk,M., Lukasova,E. and Kozubek,S. (2008) Chromatin structure influences the sensitivity of DNA to γ-radiation. *Biochim. Biophys. Acta*, **1783**, 2398–2414.
10. Guenatri,M., Bailly,D., Maison,C. and Almouzni,G. (2004) Mouse centric and pericentric satellite repeats form distinct functional heterochromatin. *J. Cell Biol.*, **166**, 493–505.
11. Noon,A.T., Shibata,A., Rief,N., Löbrich,M., Stewart,G.S., Jeggo,P.A. and Goodarzi,A.A. (2010) 53BP1-dependent robust localized KAP-1 phosphorylation is essential for heterochromatic DNA double-strand break repair. *Nat. Cell Biol.*, **12**, 177–184.
12. Kim,J.A., Kruhlak,M., Dotiwala,F., Nussenzweig,A. and Haber,E. (2007) Heterochromatin is refractory to γ-H2AX modification in yeast and mammals. *J. Cell Biol.*, **178**, 209–218.
13. Goodarzi,A., Jeggo,P. and Lobrich,M. (2010) The influence of heterochromatin on DNA double strand break repair: Getting the strong, silent type to relax. *DNA Repair*, **9**, 1273–1282.
14. Riballo,E., Kühne,M., Rief,N., Doherty,A., Smith,G.C., Recio,M.J., Reis,C., Dahm,K., Fricke,A., Krempler,A. *et al.* (2004) A pathway of double-strand break rejoining dependent upon ATM, Artemis, and proteins locating to gamma-H2AX foci. *Mol. Cell*, **16**, 715–724.
15. Psonka-Antonczyk,K., Elsässer,T., Gudowska-Nowak,E. and Taucher-Scholz,G. (2009) Distribution of double-strand breaks induced by ionizing radiation at the level of single DNA molecules examined by atomic force microcopy. *Radiat. Res.*, **172**, 288–295.
16. Asaithamby,A., Uematsu,N., Chatterjee,A., Story,M.D., Burma,S. and Chen,D.J. (2008) Repair of HZE-particle-induced DNA double-strand breaks in normal human fibroblasts. *Radiat. Res.*, **169**, 437–446.
17. Goodarzi,A.A., Noon,A.T. and Jeggo,P.A. (2009) The impact of heterochromatin on DSB repair. *Biochem. Soc. Trans.*, **37**, 569–576.
18. Bancaud,A., Huet,S., Daigle,N., Mozziconacci,J., Beaudouin,J. and Ellenberg,J. (2009) Molecular crowding affects diffusion and binding of nuclear proteins in heterochromatin and reveals the fractal organization of chromatin. *EMBO J.*, **28**, 3785–3798.
19. Jakob,B., Scholz,M. and Taucher-Scholz,G. (2003) Biological imaging of heavy charged-particle tracks. *Radiat. Res.*, **159**, 676–684.

20. Heiss,M., Fischer,B.E., Jakob,B., Fournier,C., Becker,G. and Taucher-Scholz,G. (2006) Targeted irradiation of mammalian cells using a heavy-ion microprobe. *Radiat. Res.*, **165**, 231–239.
21. Jakob,B., Splinter,J. and Taucher-Scholz,G. (2009) Positional stability of damaged chromatin domains along radiation tracks in mammalian cells. *Radiat. Res.*, **171**, 405–418.
22. Jakob,B., Rudolph,J.H., Gueven,N., Lavin,M.F. and Taucher-Scholz,G. (2005) Live cell imaging of heavy ion induced radiation responses by beamline microscopy. *Radiat. Res.*, **163**, 681–690.
23. Jakob,B., Splinter,J., Durante,M. and Taucher-Scholz,G. (2009) Live cell microscopy analysis of radiation-induced DNA double-strand break motion. *Proc. Natl Acad. Sci. USA*, **106**, 3172–3177.
24. Tobias,F., Durante,M., Taucher-Scholz,G. and Jakob,B. (2010) Spatiotemporal analysis of DNA repair using charged particle radiation. *Mutat. Res.*, **704**, 54–60.
25. Bakkenist,C.J. and Kastan,M.B. (2003) DNA damage activates ATM through intermolecular autophosphorylation and dimer dissociation. *Nature*, **421**, 499–506.
26. Bekker-Jensen,S., Lukas,C., Kitagawa,R., Melander,F., Kastan,M.B., Bartek,J. and Lukas,J. (2006) Spatial organization of the mammalian genome surveillance machinery in response to DNA strand breaks. *J. Cell Biol.*, **173**, 195–206.
27. Shibata,A., Conrad,S., Birraux,J., Geuting,V., Barton,O., Ismail,A., Kakarougkas,A., Taucher-Scholz,G., Löbrich,M. and Jeggo,P. (2011) Factors determining DNA double strand break repair pathway choice in G2 phase. *EMBO J.*, **30**, 1079–1092.
28. Ziv,Y., Bielopolski,D., Galanty,Y., Lukas,C., Taya,Y., Schultz,D.C., Lukas,J., Bekker-Jensen,S., Bartek,J. and Shiloh,Y. (2006) Chromatin relaxation in response to DNA double-strand breaks is modulated by a novel ATM- and KAP-1 dependent pathway. *Nat. Cell Biol.*, **8**, 870–876.
29. Kruhlak,M.J., Celeste,A., Dellaire,G., Fernandez-Capetillo,O., Müller,W.G., McNally,J.G., Bazett-Jones,D.P. and Nussenzweig,A. (2006) Changes in chromatin structure and mobility in living cells at sites of DNA double-strand breaks. *J. Cell Biol.*, **172**, 823–834.
30. Costes,S.V., Ponomarev,A., Chen,J.L., Nguyen,D., Cucinotta,F.A. and Barcellos-Hoff,M.H. (2007) Image-based modeling reveals dynamic redistribution of DNA damage into nuclear sub-domains. *PLoS Comput. Biol.*, **3**, e155.
31. Rogakou,E.P., Pilch,D.R., Orr,A.H., Ivanova,V.S. and Bonner,W.M. (1998) DNA double-strand breaks induce histone H2AX phosphorylation on serine 139. *J. Cell Biol.*, **273**, 5858–5868.
32. Nakamura,A.J., Rao,V.A., Pommier,Y. and Bonner,W.M. (2010) The complexity of phosphorylated H2AX foci formation and DNA repair assembly at DNA double-strand breaks. *Cell Cycle*, **9**, 389–397.
33. Splinter,J., Jakob,B., Lang,M., Yano,K., Engelhardt,J., Hell,S.W., Chen,D.J., Durante,M. and Taucher-Scholz,G. (2010) Biological dose estimation of UVA laser microirradiation utilizing charged particle-induced protein foci. *Mutagenesis*, **25**, 289–297.
34. Falk,M., Lukasova,E., Gabrielova,B., Ondrej,V. and Kozubek,S. (2007) Chromatin dynamics during DSB repair. *Biochim. Biophys. Acta*, **1773**, 1534–1545.
35. Soutoglou,E., Dorn,J.F., Sengupta,K., Jasin,M., Nussenzweig,A., Ried,T., Danuser,G. and Misteli,T. (2007) Positional stability of single double-strand breaks in mammalian cells. *Nat. Cell Biol.*, **9**, 675–682.
36. Chiolo,I., Minoda,A., Colmenares,S.U., Polyzos,A., Costes,S.V. and Karpen,G.H. (2011) Double-strand breaks in heterochromatin move outside of a dynamic HP1a domain to complete recombinational repair. *Cell*, **144**, 732–744.